Thermochimica Acta, 206 (1992) 219–234
Elsevier Science Publishers B.V., Amsterdam

Thermoanalytical study of $La_2Ni_xCu_{1-x}O_4$ preparation from mixed nitrates of lanthanum, nickel and copper

Tiberius C. Vaimakis

University of Ioannina, Chemistry Department, P.O. Box 1186, 45110 Ioannina (Greece)

(Received 25 October 1991)

Abstract

The thermal decomposition of $La(NO_3)_3 \cdot 6H_2O$, $Ni(NO_3)_2 \cdot 6H_2O$ and $Cu(NO_3)_2 \cdot 3H_2O$, and their mixtures with molar ratios such as are required for the formation of the perovskite series $La_2Ni_xCu_{1-x}O_4$ ($x = 0$, 0.2, 0.4, 0.6, 0.8 and 1), was studied using a thermogravimetric continuous mode method and a batch method, the mixtures being heated at appropriately chosen temperatures. The batches after cooling were examined by X-ray diffraction (XRD) and IR spectrometry to identify the intermediate and final products. From the thermogravimetric results the kinetic parameters of decomposition were calculated by the Coats–Redfern method using various mechanisms.

The experimental results for the mixtures show that the production of the perovskite phases takes place through the formation of the basic nitrate–hydrate salts at first, and subsequently the oxynitrate salts. The predominant mechanism of formation of the oxynitrate salts is chemical reaction with activation energies substantially less than that of the raw materials. It should be noted that the compensation effect is observed.

INTRODUCTION

One of the methods for the synthesis of perovskite materials is the precursor solid solution method, which has several advantages because the reacting cations are uniformly blended together, avoiding diffusion problems and the products formed at lower temperatures. Thus, they have large specific surface areas which are important to catalytic materials [1]. Unfortunately, precursor solid solutions have not always been found possible. Mixed nitrates, however, seem to be useful in preparing perovskites which require low temperature thermal treatment [2].

The thermal treatment of single compounds, lanthanum nitrate hexahydrate [3–7], nickel nitrate hexahydrate [8–11] and copper nitrate trihydrate [12] has been studied previously. The thermal decomposition of hydrated nitrate salts began at low temperatures (50–70°C) with dehydration gradu-

Correspondence to: T.C. Vaimakis, University of Ioannina, Chemistry Department, P.O. Box 1186, 45110 Ioannina, Greece.

ally to the di- and monohydrate up to 200–220°C. Further increase in temperature led first to the formation of basic nitrate salts, and then to simple and/or complex oxynitrate salts as intermediate thermal decomposition products. Finally, the oxynitrate salts decomposed at higher temperatures, giving oxides. Information on the thermal decomposition process of mixed nitrate salts is absent, and so the choice of the sintering conditions is empirical.

In the present paper, on the basis of thermal analysis and infrared spectroscopic data, we studied the mechanism and the kinetics of the thermal decomposition of $La(NO_3)_3 \cdot 6H_2O$–$Ni(NO_3)_2 \cdot 6H_2O$–$Cu(NO_3)_2 \cdot 3H_2O$ mixtures in molar ratios that correspond to the composition of the $La_2NI_xCu_{1-x}O_4$ system (where $x = 0.0$, 0.2, 0.4, 0.6, 0.8 and 1.0).

EXPERIMENTAL AND RESULTS

The raw materials used in the study were $La(NO_3)_3 \cdot 6H_2O$, $Ni(NO_3)_2 \cdot 6H_2O$ and $Cu(NO_3)_2 \cdot 3H_2O$ (Ferak, analytical reagents). Mechanical mixtures with molar ratios of the nitrate salts lanthanum : nickel : copper equal to 2.0 : 1.0 : 0.0, 2.0 : 0.8 : 0.2, 2.0 : 0.6 : 0.4, 2.0 : 0.4 : 0.6, 2.0 : 0.2 : 0.8 and 2.0 : 0.0 : 1.0 (which we designate LN, LNC82, LNC64, LNC46, LNC28 and LC mixtures correspondingly) were prepared by mixing in a porcelain mortar under strong grinding.

The thermal analysis of the above mixtures as well as the raw materials was carried out using a Chyo-TRDA$_3$H derivatograph with simultaneous recording of temperature (T), thermogravimetry (TG), differential thermogravimetry (DTG) and differential thermal analyses (DTA). All the analysis used α-Al_2O_3 as a blank and a heating rate of 1.46°C min^{-1} with a nitrogen flow of 5 l h^{-1}. Figure 1 illustrates the TG, DTG and DTA curves of $La(NO_3)_3 \cdot 6H_2O$, $Ni(NO_3)_2 \cdot 6H_2O$ and $Cu(NO_3)_2 \cdot 3H_2O$. Figure 2 illustrates the TG, DTG and DTA curves of the prepared mixtures.

Samples ($\approx$ 15 g) from the LN and LC mixtures were heated in porcelain crucibles at 165, 275, 345 and 550°C the first one and at 240, 380 and 550°C the second for 2 h at each temperature. IR spectra of the samples from batch experiments were recorded with a Perkin-Elmer 783 spectrophotometer and are shown in Fig. 3.

Samples ($\approx$ 10 g) of all ternary mixtures were heated in a porcelain crucible at 550°C for 2 h. The X-ray diffraction (XRD) patterns of the thermal decomposition products and also the products from the LN and LC mixtures which were heated at 550°C were obtained using a Siemens D-500 diffractometer with Cu Kα radiation (λ = 1.54060 Å), and are illustrated in Fig. 4.

Another series of mechanical mixtures ($\approx$ 15 g) was heated initially at 850°C for 2 h and, after grinding, at 1050°C, also for 2 h. The XRD patterns of both series of thermal decomposition products so prepared,

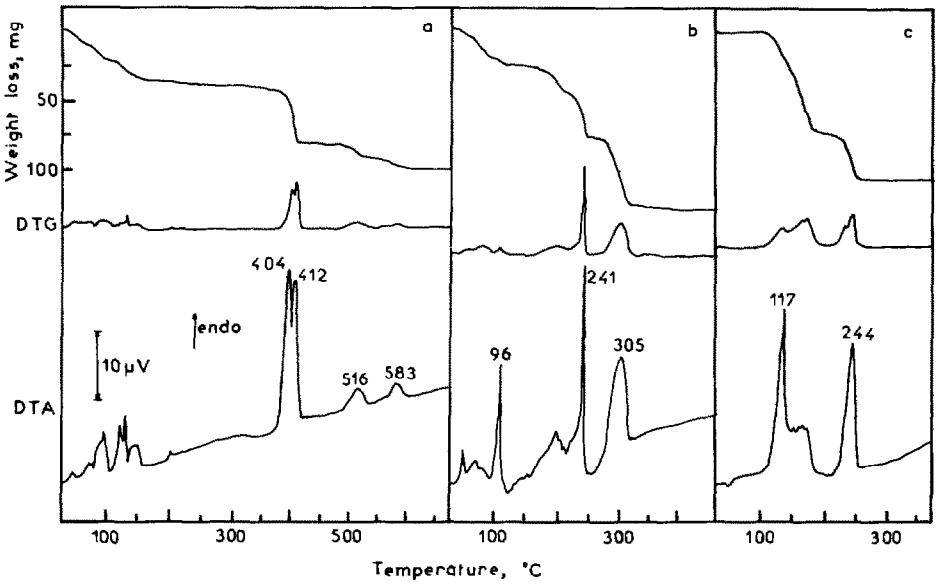

Fig. 1. TG, DTG and DTA curves of raw materials with heating rate 1.46°C min^{-1}. (a) Sample $La(NO_3)_3 \cdot 6H_2O$ and sample weight 151.4 mg; (b) sample $Ni(NO_3)_2 \cdot 6H_2O$ and sample weight 141.9 mg; (c) sample $Cu(NO_3)_2 \cdot 3H_2O$ and sample weight 151.0 mg.

were recorded using a Philips system (PW 2253 lamp, PW 1050 goniometer, PW 1965/50 analogue detector) with Co Kα radiation ($\lambda = 1.7902$ Å), and are illustrated in Fig. 5.

The kinetics of the thermal decomposition of the raw materials and the obtained mixtures were studied using the modified Coats–Redfern method, based on eqn. (1), for various mechanisms [13] as listed in Table 1

$$\ln\left[\frac{f(\alpha)}{T^2}\right] = \ln\left[\frac{ZR}{\beta E_a}\left(1 - \frac{2RT}{E_a}\right)\right] - \frac{E_a}{RT} \tag{1}$$

where $f(\alpha)$ is the integral of the inverse function which describes the dependence of $d\alpha/dt$ on α, α is the reacted molar fraction, t is the time, T is the temperature, Z is the pre-exponential factor, R is the gas constant, E_a is the activation energy and β is the heating rate. When $\ln[f(\alpha)/T^2]$ is plotted against $1/T$, straight lines can be drawn by the method of least squares, from which E, Z and the correlation coefficient r are calculated. The reaction order n, for the n-order reaction model, which yields the highest correlation coefficient is accepted as representing the best reaction order. Independently of the value of the best reaction order are also calculated the kinetic parameters of the chemical reaction model for $n = 0$, 1/2, 2/3, 1, 2 and 3 which have theoretical significance. The calculated values of the E, Z and r of single salts and their mixtures are shown in Tables 2 and 3 correspondingly for various reaction models.

DISCUSSION

Raw materials

The thermal decomposition of $La(NO_3)_3 \cdot 6H_2O$, as shown in Fig. 1a, is very complicated and takes place in three main steps. The first step is made up of several not very distinct stages with a total weight loss of about 24.2%, and corresponds to removal of the six crystal water molecules.

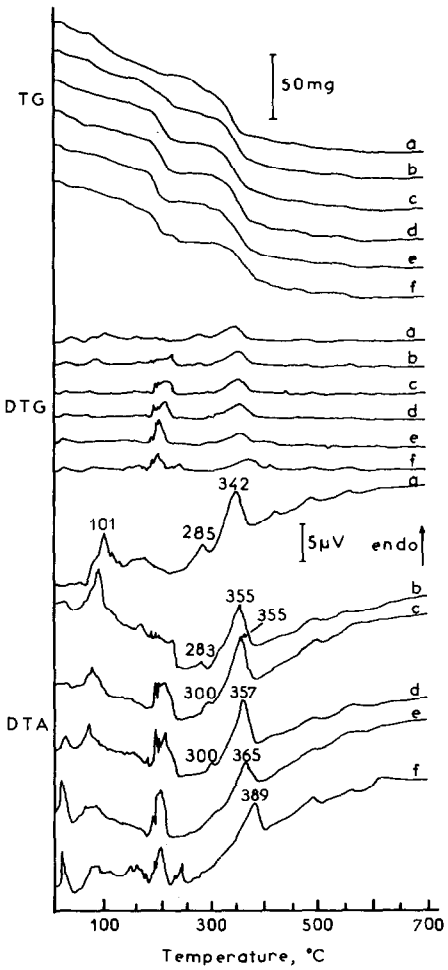

Fig. 2. TG, DTG and DTA curves of mixtures with heating rate 1.46°C min^{-1}. Curve a, sample LN and sample weight 150.5 mg; curve b, sample LNC82 and sample weight 151.2 mg; curve c, sample LNC64 and sample weight 151.3 mg; curve d, sample LNC46 and sample weight 150.6 mg; curve e, sample LNC28 and sample weight 149.8 mg; curve f, sample LC and sample weight 146.8 mg.

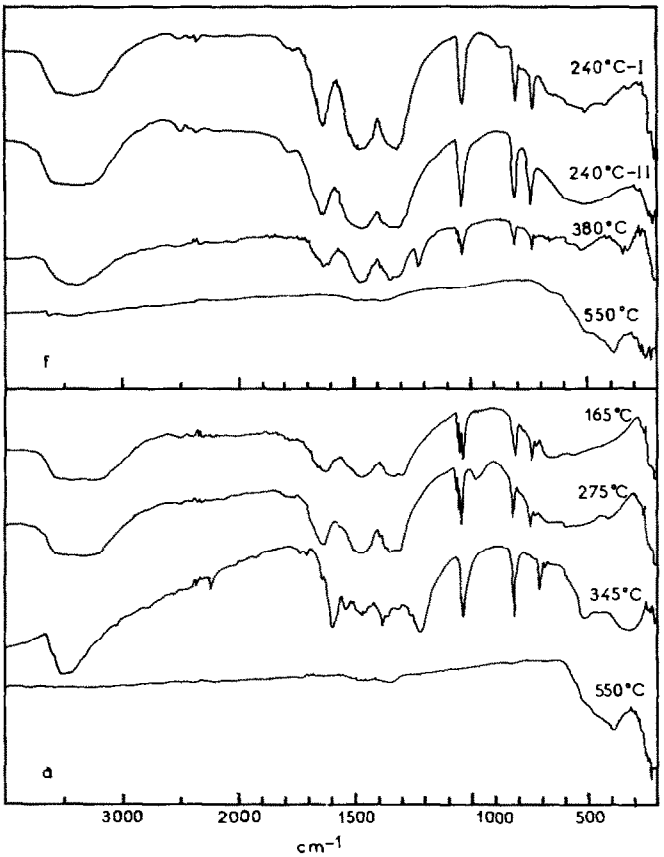

Fig. 3. IR spectra of LN (a) and LC (f) mixtures heated at the temperatures indicated.

The second step takes place between 300 and 460°C and consists of two overlapping strongly endothermic stages with corresponding peak maxima at 404 and 412°C. The weight loss is about 25.9% and corresponds to the decomposition reaction

$$La(NO_3)_3 \rightarrow LaO(NO_3) + N_2O_5 \quad (2)$$

Table 2 contains the kinetic parameters obtained when eqn. (1) was applied to the data with the different expressions for $f(\alpha)$. The results show that all the reaction mechanisms give markedly different activation energies and that the mechanisms F0.1 and D1 have the best correlation coefficients (0.99101 and 0.99129 respectively) with E_a equal to 77.4 and 152.9 kcal mol^{-1} and ln Z equal to 54.8 and 111 respectively. According to Strydom and Van Vuuren [6], the calculated activation energy of this stage was 54 kcal mol^{-1} by the R2 mechanism for isothermal conditions and 29.4 kcal mol^{-1} from the DSC trace, which agrees with the value we calculated for the A3 mechanism (32.2 kcal mol^{-1}). Belov et al. [14] calculated the kinetic parameters for the overall process using the same method as ours,

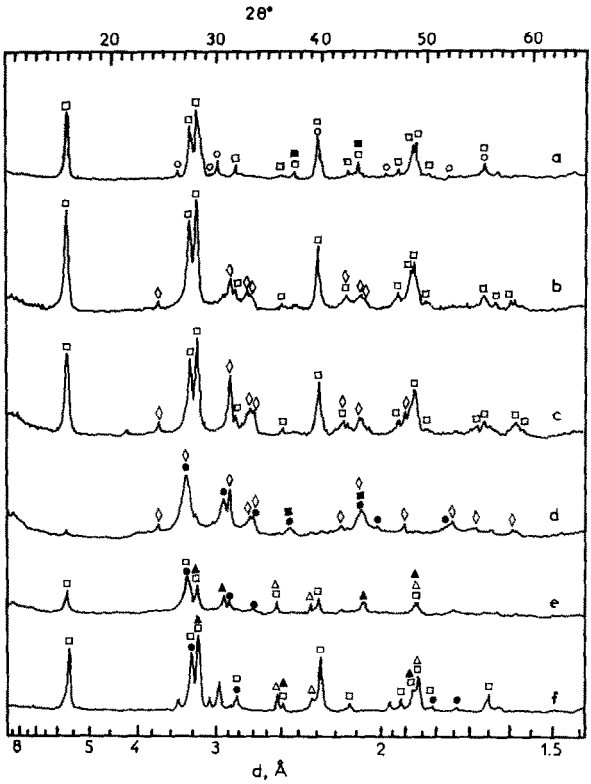

Fig. 4. XRD patterns of the mixtures heated at 550°C with sample indication letters for curves as for Fig. 2. (○) La_2O_3 5-0602, (●) La_2O_3 22-0369, (□) $La(OH)_3$ 36-1481, (■) NiO 22-1189, (△) CuO 5-0661, (▲) Cu_4O_3 33-0480 and (◇) $CuLa_2O_4$ 30-0487. (Radiation Cu Kα; numbers from ASTM data files.)

and at a heating rate of 5°C min^{-1} they found $E = 2.9$ kcal mol^{-1}, ln $Z = -1.4$ and $n = 0.83$.

The third step showed weight loss starting at 480°C and involved two successive endothermic stages with maximum rate of transformation at 516 and 583°C correspondingly. The weight losses were about 6.0% and 5.9% and they corresponded to the decomposition reactions

$$4LaO(NO_3) \rightarrow 2LaO(NO_3) \cdot La_2O_3 + N_2O_5 \quad (3)$$

$$2LaO(NO_3) \cdot La_2O_3 \rightarrow 2La_2O_3 + N_2O_5 \quad (4)$$

Figure 1, curve b shows the thermal decomposition of $Ni(NO_3)_2 \cdot 6H_2O$, which takes place in three main steps. The first step begins at 35°C and comprises several undifferentiated stages with a sharp endothermic stage at 96°C. The total weight loss is 14.7% and corresponds to removal of 2.33 crystal water molecules.

The second step is made up of two stages. One stage with a weight loss of about 11% corresponds to the production of $Ni(NO_3)_2 \cdot 2H_2O$. The next

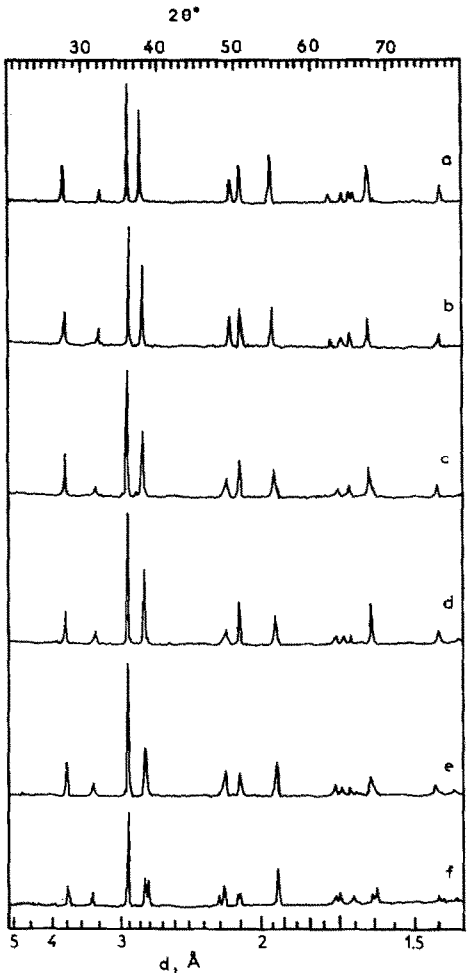

Fig. 5. XRD patterns of the mixtures heated at 1050°C with sample indication letters for curves as for Fig. 2. (Radiation Co Kα.)

stage, with a sharp endothermic peak at 241°C and a weight loss of 18.8%, is followed by a small plateau. Up to this plateau the total weight loss is 44.5%, which corresponds to the production of the basic nitrate salt, either $2Ni(NO_3)_2 \cdot Ni(OH)_2$ (theoretical weight loss 47.48%) according to Paulik et al. [9], or $Ni(NO_3)_2 \cdot 2Ni(OH)_2 \cdot 4H_2O$ (theoretical weight loss 49.54%) according to Gadalla and Yu [10].

$$Ni(NO_3)_2 \cdot 2H_2O \rightarrow (1/3)[2Ni(NO_3)_2 \cdot Ni(OH)_2] + (1/3)N_2O_5 + (5/3)H_2O \quad (5)$$

$$Ni(NO_3)_2 \cdot 2H_2O \rightarrow (1/3)[Ni(NO_3)_2 \cdot 2Ni(OH)_2 \cdot 4H_2O] + (2/3)N_2O_5 \quad (6)$$

TABLE 1

Classification of solid state rate expressions

Symbol		$f(\alpha)$
Acceleratory α–time curves		
Pn	Power law ($n = 1, 2, 3$ and 4)	$\alpha^{1/n}$
Sigmoid α–time curves		
A2	Avrami–Erofe'ev (Random nucleation)	$[-\ln(1-\alpha)]^{1/2}$
A3	Avrami–Erofe'ev (Random nucleation)	$[-\ln(1-\alpha)]^{1/3}$
A4	Avrami–Erofe'ev (Random nucleation)	$[-\ln(1-\alpha)]^{1/4}$
Deceleration α–time curves based on geometrical models		
R2	Contracting area	$1-(1-\alpha)^{1/2}$
R3	Contracting volume	$1-(1-\alpha)^{1/3}$
Deceleration α–time curves based on diffusion mechanisms		
D1	One-dimensional	α^2
D2	Two-dimensional	$(1-\alpha)\ln(1-\alpha)+\alpha$
D3	Three-dimensional, spherical symmetry; Jander equation	$[1-(1-\alpha)^{1/3}]^2$
D4	Three-dimensional, spherical symmetry; Ginstling–Brounshtein equation	$(1-2\alpha/3)-(1-\alpha)^{2/3}$
Deceleration α–time curves based on order of reaction		
F1	First order	$-\ln(1-\alpha)$
Fn	nth-order ($n = 0, 1/2, 2/3, 2, 3$)	$[1-(1-\alpha)^{1-n}]/(1-n)$

Table 2 contains the kinetic parameters of the sharp endothermic stage for the different expressions of $f(\alpha)$. The results are proportionate to the second step of $La(NO_3)_2 \cdot 6H_2O$ decomposition with activation energies smaller than these by about 15–20%. The mechanism F1.3 gave the best correlation coefficient (0.98827) with E_a equal to 86.8 kcal mol^{-1} and ln Z equal to 84.2.

The third step is simple, with a maximum rate of conversion at 305°C, and leads to formation of NiO

$$2Ni(NO_3)_2 \cdot Ni(OH)_2 \rightarrow 3NiO + 2N_2O_5 + H_2O \quad (7)$$

$$Ni(NO_3)_2 \cdot 2Ni(OH)_2 \cdot 4H_2O \rightarrow 3NiO + N_2O_5 + 6H_2O \quad (8)$$

The kinetic parameters are shown in Table 2. The best correlation coefficient is given by the F1.5 mechanism (0.99894) with activation energy equal to 59.1 kcal mol^{-1} and ln Z equal to 50.0. These values agree with the calculated kinetic parameters ($n = 1.5$, $E_a = 62.9$ kcal mol^{-1} and ln $Z = 50.5$) from Popescu et al. [11] for the reaction

$$Ni(NO_3)_2 \rightarrow NiO + 2NO_2 + (1/2)O_2 \quad (9)$$

TABLE 2

Kinetic parameters for the decomposition of $La(NO_3)_3 \cdot 6H_2O$, $Ni(NO_3)_2 \cdot 6H_2O$ and $Cu(NO_3)_2 \cdot 3H_2O$

	$La(NO_3)_3 \cdot 6H_2O$ Second step			$Ni(NO_3)_2 \cdot 6H_2O$						$Cu(NO_3)_2 \cdot 3H_2O$ Second step		
				Second step			Third step					
	E	$\ln Z$	r	E	$\ln Z$	r	E	$\ln Z$	r	E	$\ln Z$	r
P1	75.1	53.1	0.99098	66.6	63.4	0.97224	41.9	33.8	0.98008	40.3	37.1	0.95380
P2	36.2	23.9	0.99031	32.3	29.2	0.97053	19.8	14.1	0.97771	19.1	15.8	0.94907
P3	23.3	14.0	0.98957	20.9	17.6	0.96866	12.5	7.4	0.97492	12.1	8.6	0.94362
P4	16.8	8.9	0.98873	15.2	11.7	0.96661	8.8	4.0	0.97160	8.6	4.9	0.93729
A2	49.6	34.3	0.98475	39.7	36.9	0.98674	25.1	19.2	0.99610	26.9	24.0	0.98495
A3	32.2	21.0	0.98393	25.8	22.8	0.98605	16.0	10.8	0.99568	17.2	14.2	0.98374
A4	23.5	14.3	0.98304	18.8	15.6	0.98530	11.4	6.6	0.99520	12.4	9.2	0.98238
R2	87.4	61.9	0.98987	73.4	69.7	0.98177	46.6	37.6	0.98984	47.2	43.6	0.97258
R3	92.0	65.0	0.98878	75.9	71.9	0.98416	48.4	38.9	0.99246	49.9	46.0	0.97776
D1	152.9	111	0.99129	135.3	131	0.97304	86.0	72.5	0.98113	82.6	78.8	0.95592
D2	168.0	122	0.99094	143.6	139	0.97914	91.8	77.3	0.98709	91.0	86.8	0.96725
D3	186.6	134	0.98908	153.8	148	0.98457	99.1	82.6	0.99283	101.8	96.4	0.97863
D4	174.1	125	0.99049	146.9	141	0.98124	94.2	78.0	0.98926	94.5	88.9	0.97153
F0	77.1	53.1	0.99098	66.6	63.4	0.97224	41.9	33.8	0.98008	40.3	37.1	0.95380
$F\frac{1}{2}$	87.4	62.6	0.98987	73.4	70.4	0.98177	46.6	38.3	0.98984	47.2	44.3	0.97258
$F\frac{2}{3}$	92.0	66.1	0.98878	75.9	73.0	0.98416	48.4	40.0	0.99246	49.9	47.0	0.97776
F1	101.9	73.7	0.98551	81.4	78.6	0.98739	52.4	43.7	0.99647	55.7	53.1	0.98603
F2	138.0	101	0.96901	101.4	99.2	0.98278	66.7	57.2	0.99724	77.7	75.7	0.99368
F3	182.2	135	0.94943	125.8	124	0.96268	84.2	73.6	0.98557	104.9	104	0.98532
Fn	($n = 0.1$)			($n = 1.3$)			($n = 1.5$)			($n = 1.8$)		
	77.4	54.8	0.99101	86.8	84.2	0.98827	59.1	50.0	0.99894	72.8	70.7	0.99396

TABLE 3

Kinetic parameters for the second step of decomposition of the $La(NO_3)_3 \cdot 6H_2O$, $Ni(NO_3)_2 \cdot 6H_2O$ and $Cu(NO_3)_2 \cdot 3H_2O$ mixtures

	Composition of mixtures La:Ni:Cu											
	2:1:0						2:0.8:0.2			2:0.6:0.4		
	Stage I			Stage II								
	E	ln Z	r	E	ln Z	r	E	ln Z	r	E	ln Z	r
P1	34.2	28.2	0.99058	18.8	11.0	0.83892	17.6	10.5	0.98564	22.7	14.7	0.99438
P2	16.0	11.2	0.98918	8.2	2.3	0.79939	7.6	2.1	0.98046	10.2	4.2	0.99277
P3	10.0	5.4	0.98748	4.6	−0.5	0.74639	4.3	−0.6	0.97224	6.0	0.7	0.99047
P4	6.9	2.5	0.98536	2.8	−0.1	0.67485	2.6	0.9	0.95818	3.9	−0.9	0.98700
A2	20.8	16.1	0.99807	12.6	6.4	0.90226	10.8	5.2	0.98993	13.5	7.4	0.99536
A3	13.2	8.8	0.99786	7.5	2.1	0.88237	6.4	1.4	0.98760	8.2	2.8	0.99460
A4	9.4	5.0	0.99762	5.0	0.05	0.85657	4.2	−0.5	0.98430	5.6	0.5	0.99360
R2	38.5	31.8	0.99674	22.6	13.8	0.87927	20.3	12.4	0.99253	25.7	16.8	0.99785
R3	40.2	33.1	0.99784	24.2	14.8	0.89259	21.4	13.1	0.99328	26.9	17.4	0.99790
D1	70.4	61.4	0.99118	40.2	27.9	0.85487	37.4	26.7	0.98753	47.7	34.9	0.99500
D2	75.8	66.0	0.99512	44.6	31.2	0.87576	40.8	29.1	0.99162	51.4	37.5	0.99729
D3	82.5	71.1	0.99796	50.8	35.1	0.90183	45.2	31.8	0.99395	56.1	40.3	0.99806
D4	78.0	66.6	0.99637	46.6	31.4	0.88499	42.2	28.9	0.99285	52.9	37.4	0.99786
F0	34.2	28.2	0.99058	18.8	11.0	0.83892	17.6	10.5	0.98564	22.7	14.7	0.99438
$F\frac{1}{2}$	38.5	32.5	0.99674	22.6	14.5	0.87927	20.3	13.1	0.99253	25.7	17.4	0.99785
$F\frac{2}{3}$	40.2	34.2	0.99784	24.2	15.9	0.89259	21.4	14.2	0.99328	26.9	18.5	0.99790
F1	43.8	37.8	0.99825	27.6	19.0	0.91782	24.0	16.6	0.99162	29.4	20.9	0.99596
F2	57.4	51.2	0.98504	41.5	31.2	0.97074	33.9	25.9	0.96280	39.2	29.8	0.97423
F3	74.2	67.7	0.96051	59.1	46.6	0.99043	46.5	37.4	0.92483	51.3	40.6	0.94286
Fn	($n = 0.9$)			($n = 4.8$)			($n = 0.7$)			($n = 0.6$)		
	42.7	36.6	0.99839	95.2	78.0	0.99614	21.7	14.4	0.99331	26.4	18.1	0.99796

Finally, Belov et al. [14] calculated the kinetic parameters for the overall process of the decomposition of $Ni(NO_3)_2 \cdot 6H_2O$ and they found $E_a = 7.5$ kcal mol^{-1}, ln $Z = 5.1$ and $n = 1.19$.

The thermal decomposition of $Cu(NO_3)_2 \cdot 3H_2O$ takes place, as is shown in Fig. 1, curve c, in two main steps. The first step is complicated and is made up of a sharp endothermic peak at 117°C followed by two or more indistinct small peaks. The weight loss is 45.1%, which corresponds to production of the oxynitrate salt $Cu_2O(NO_3)_2$ (theoretical 44.7%).

The formation of CuO at the end of the second step seems to take place in two stages (DTG curve) with a sharp endothermic peak at 244°C. The kinetic parameters for the reaction (10) are given in Table 2. The best correlation coefficient is given by the F1.8 mechanism (0.99396) with

2:0.4:0.6			2:0.2:0.8			2:0:1		
E	ln Z	r	E	ln Z	r	E	ln Z	r
26.0	17.4	0.96326	20.2	12.6	0.98405	26.9	17.5	0.99200
11.8	5.6	0.95525	8.9	3.1	0.97906	12.2	5.7	0.99007
7.0	1.6	0.94456	5.1	−0.01	0.97158	7.3	1.7	0.98743
4.6	−0.3	0.92988	3.2	−1.1	0.95977	4.9	−0.3	0.98370
18.2	11.5	0.99494	13.1	7.1	0.99775	16.3	9.4	0.99833
11.3	5.6	0.99409	7.9	2.6	0.99728	10.0	4.2	0.99810
7.9	2.6	0.99302	5.4	0.4	0.99664	6.9	1.5	0.99782
31.5	21.6	0.98318	23.9	15.3	0.99450	30.6	20.0	0.99794
33.8	23.2	0.98836	25.3	16.2	0.99659	32.0	20.8	0.99880
54.4	40.3	0.96651	42.8	30.8	0.98594	56.4	40.5	0.99278
60.9	45.2	0.97767	47.2	34.1	0.99196	60.8	43.6	0.99649
70.0	51.6	0.98922	53.1	37.9	0.99694	66.4	47.0	0.99890
63.9	46.3	0.98217	49.1	34.3	0.99409	62.6	43.7	0.99763
26.0	17.4	0.96326	20.2	12.6	0.98405	26.9	17.5	0.99200
31.5	22.3	0.98318	23.9	16.0	0.99450	30.6	20.7	0.99794
33.8	24.2	0.98836	25.3	17.3	0.99659	32.0	21.9	0.99880
38.8	28.7	0.99564	28.6	20.3	0.99811	35.0	24.6	0.99851
59.2	46.3	0.99284	41.5	31.8	0.98321	46.6	34.6	0.98168
85.1	68.6	0.97474	57.6	46.2	0.95831	60.8	46.8	0.95368
(n = 1.4)			(n = 1.0)			(n = 0.8)		
46.1	35.0	0.99843	28.6	20.3	0.99811	33.2	23.0	0.99902

activation energy equal to 72.8 kcal mol^{-1} and ln Z equal to 70.7. Belov et al. [14] calculated the kinetic parameters for the overall process and found E = 7.2 kcal mol^{-1}, ln Z = 4.9 and n = 0.14.

$$Cu_2O(NO_3)_2 \rightarrow 2CuO + N_2O_5 \quad (10)$$

In Fig. 6a is illustrated the plot of ln Z against E_a for all the mechanisms of the raw materials. The compensation effect is

$$\ln Z = a + bE \quad (11)$$

observed for the decomposition of lanthanum nitrate salt, giving coefficients of the compensating equation (11) $a = -2.9761$ and $b = 0.74490$ (line 1), for the second step of the nickel nitrate and copper nitrate salts $a = -2.8072$ and $b = 0.99138$ (line 2), and for the third step of the nickel nitrate salt $a = -3.1311$ and $b = 0.99650$ (line 3).

Mixtures

The thermal decomposition curves of the mixtures are shown in Fig. 2. The TG curves indicate that the processes take place in two main steps.

The first step is very complicated, as shown from the DTG and DTA curves. The decomposition begins at about 50°C with a low decomposition rate, which decreases at the end of the steps at about 225–250°C. The weight losses are 25.0, 28.6, 29.3, 29.2, 29.0 and 32.1% for the LN, LNC82, LNC64, LNC46, LNC28 and LC mixtures respectively. Comparison of these values with the results for the raw materials indicates that the products from the initial salts are the compounds $La(NO_3)_3$, $Ni(NO_3)_2 \cdot 2H_2O$ and $Cu(OH)_2$ in the same proportion as for the corresponding salts in the mixtures. (The theoretical weight losses are 24.91%, 26.43%, 27.95%, 29.48%, 31.00% and 32.52% in the same series as for the above mentioned mixtures.)

$$2[La(NO_3)_3 \cdot 6H_2O] + (1-x)[Ni(NO_3)_2 \cdot 6H_2O] + x[Cu(NO_3)_2 \cdot 3H_2O]$$
$$\rightarrow 2La(NO_3)_3 \cdot (1-x)[Ni(NO_3)_2 \cdot 2H_2O] \cdot xCu(OH)_2$$
$$+ xN_2O_5 + (14-2x)H_2O \qquad (12)$$

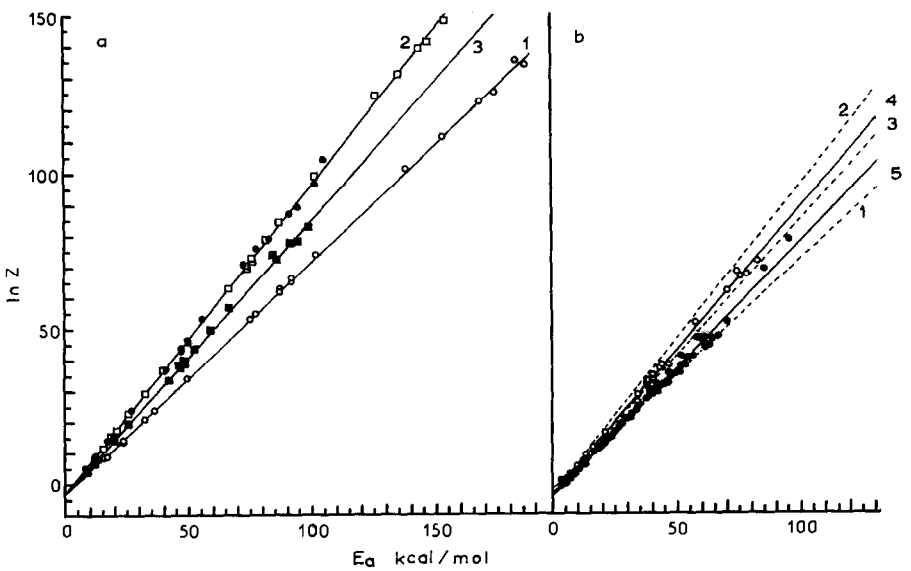

Fig. 6. Compensation effect between the parameters ln Z and E_a: (a) raw materials and (b) mixtures. (1) Second step for lanthanum nitrate, (2) second step for nickel and copper nitrates, (3) third step for nickel nitrate, (4) state I of second step for the LN mixture, and (5) stage II of second step for the mixtures.

The same results are indicated also by the IR spectra (Fig. 3) for the first and the last terms of the series of mixtures (LN and LC mixtures) at 165 and 240°C correspondingly. The product of thermal decomposition at 240°C of the lanthanum–copper nitrate mixture had two phases, one green (I-phase) and the other grey (II-phase) in colour, the IR spectra of which were taken separately. The broad absorption band at 3600–3000 cm^{-1} (stretching), with the absorptions at 662 for the LN mixture and 667 cm^{-1} (libration modes) for the I-phase of the LC mixture, indicates the presence of crystal water molecules. The bending in-plane vibration of the water molecules is overlapped by the stretching vibration of the N=O group so that it appears as a shoulder peak at 1652 cm^{-1} for the LN mixture and 1650 cm^{-1} for the I-phase of the LC mixture. The nitrate group absorbs at a large number of band positions which are observed in our case; it is interesting to note, for the LN mixture, the triple peak (1051, 1043 and 1030 cm^{-1}) for the symmetric stretching vibration of the NO_2 group, which indicates that there are three different nitrate ions in the heated sample. The presence of a broad band at 1520–1435 cm^{-1} is characteristic for the antisymmetric stretching vibration of NO_2 of the monodentate nitrate group. However, absorption in the ≈ 1600 cm^{-1} region, characteristic of the stretching vibration of N=O of the bidentate nitrate group, is absent. The absorptions at 510, 430 and 325 cm^{-1} for the I-phase of the LC mixture are the vibration modes of the Cu–OH and Cu–O groups.

The second steps comprise two endothermic stages followed by a gradual loss in weight up to 620°C. The weight loss is 38.3% for the LN mixture and decreases gradually (34.8%, 33.8%, 33.5%, 33.2%) to 29.8% as the content of nickel nitrate salt in the initial mixtures is decreased (LC mixture). The weight losses of the first stages decrease also gradually up to disappearance with the decreasing concentration in the initial mixtures of the nickel nitrate salt.

The weight loss of the first stage for the LN mixture is calculated from the TG curve as a value of 8.75%, which corresponds to the formation of $Ni(NO_3)_2 \cdot 2Ni(OH)_2$ from $Ni(NO_3)_2 \cdot 2H_2O$. This stage begins at 225°C with a maximum rate of transformation at 285°C. When the mixture is heated at 275°C the IR spectrum is the same as that after heating at 165°C, and has only two new absorption bands, one at 973 cm^{-1} (δ(MOH)) and another at 390 cm^{-1} (ν_{as}(MO)).

The kinetic parameters are shown in Table 3 stage I. The best correlation coefficient is given by the F0.9 mechanism (0.99839) with activation energy equal to 42.7 kcal mol^{-1} and ln Z equal to 36.6. The calculated activation energy is half of that at stage I of the nickel nitrate salt (86.8 kcal mol^{-1}); however, the temperature for the maximum transformation rate is 44°C higher than for the single salt (241°C).

The second stages have a mean weight loss value of about 22%, which corresponds to the formation of $La_2Ni_{(1-x)}Cu_xO_{3.5}(NO_3)$ compounds. The

temperature of the maximum rate of transformation is 342°C for the LN mixture and increases gradually as the concentration of nickel nitrate salt is decreased (355, 355, 357, 365 and 389°C).

The IR spectra of LN and LC mixtures, with heating temperature 345 and 380°C respectively (Fig. 3), show different results. In the spectrum of the LN mixture there is one type of nitrate group, a single absorption peak at 1038 cm^{-1} ($\nu_s(NO_2)$) and a sharp absorption peak at 817 cm^{-1} ($\delta(NO_2)$), absorption of nitric oxides (2235, 2045, 1933, 1735, 1540, 1261, 1229, 1217 and 527 cm^{-1}, according to the literature [15,16]) and moisture (3570–3060 cm^{-1} broad band, 1640 cm^{-1} shoulder and 684 cm^{-1}). The spectrum of the LC mixture shows that there are three types of nitrate ion, with a triple peak at 1052, 1043 and 1030 cm^{-1}, and indications for absorption of NO_2 (1213 cm^{-1}) and the perovskite phase La_2CuO_4 (677, 527 and 343 cm^{-1} according to the literature [17,18]).

The kinetic parameters of this stage for all the mixtures are shown in Table 3. The predominant mechanism is the Fn, with reaction order, apart from stage II of the LN mixture, of about 0.9 (0.6–1.4) and activation energy about 31 kcal mol^{-1} (21.7–46.1 kcal mol^{-1}). This mean value of E_a is much less than those for the raw materials (59.1–77.4 kcal mol^{-1}). For the LN mixture stage II, the kinetic parameters for the Fn mechanism are $n = 4.8$ and $E_a = 95.2$ kcal mol^{-1}.

The mixtures are heated at 550°C to complete the decomposition. The IR spectrum of the LN mixture (Fig. 3) shows that only the oxide is formed, without the La_2NiO_4 phase; features absent are the characteristic deformation vibration of the bridging Ni–O–Ni bond, according to Savchenko et al. [19], at 670 cm^{-1} and the stretching vibration of the La–O bond, according to Odier et al. [20], at 660 cm^{-1}, and also indications of absorbed NO_2 from the very weak broad band at 1488–1345 cm^{-1}. The IR spectrum of the LC mixture (Fig. 3) shows the previously mentioned absorptions of the La_2CuO_4 phase (677, 527 and 343 cm^{-1}) as shoulder peaks on the strong absorption band of La_2O_3 at 350–500 cm^{-1}, and also the presence of traces of the absorption of NO_2 (very weak broad band at 1341–1517 cm^{-1}) and humidity (3590 and 3370 cm^{-1}).

The XRD patterns of the heated mixtures at 550°C are shown in Fig. 4. They indicate mainly the oxides of the metals and the $La(OH)_3$ phase which were produced by reaction of La_2O_3 with moisture. Of the perovskite phases, only La_2CuO_4 is present in the samples of LNC46, LNC64 and LNC28 mixtures.

The XRD patterns of the heated mixtures at 1050°C are shown in Fig. 5. They indicate that the perovskite phases are well crystallized. In particular, the XRD patterns of the heated samples of the LN and LC mixtures agree with those in the literature: refs. 21 and 22 respectively.

The compensation effect between the pre-exponential factor (Z) and the activation energy E_a for the decomposition of all the mixtures is depicted

in Fig. 6b. For stage I of decomposition of the LN mixture the coefficients of the compensating equation are $a = -3.3367$ and $b = 0.92168$ (line 4) and those for stage II of all the mixtures are $a = -3.9241$ and $b = 0.81619$ (line 5). In Fig. 6b are also shown the lines 1, 2 and 3 from Fig. 6a. From Fig. 6 we conclude that stage II of the second step for the mixtures involves the same main mechanism, which is possibly that of eqn. (2).

CONCLUSIONS

The thermogravimetric study of the decomposition of mixtures of lanthanum, nickel and copper nitrate–hydrate salts shows that this occurs mainly in two steps. The first one leads to formation of the basic nitrate salts with crystalline water molecules. In the second step there is a rapid stage which leads to the formation of oxynitrate salts followed by a slow stage. Perovskite phases begin to be formed at the end of the weight loss, that is, at about 550°C.

The predominant mechanism of the rapid stage of the second step is chemical reaction with reaction order 0.9 and activation energy 31 kcal mol^{-1}, a value substantially lower than that for the raw materials. The compensation effect is observed for this stage.

REFERENCES

1 C.N.R. Rao and J. Gopalakrishnan, New Directions in Solid State Chemistry, Cambridge Solid State Science Series, Cambridge University Press, New York, 1989, p. 119.
2 Ref. 1, p. 488.
3 W.W. Wendlandt, Anal. Chim. Acta, 15 (1956) 435.
4 A.K. Molodkin, Z.K. Odinets, O.Vargas Ponse and B.E. Zaitsev, Zh. Neorg. Khim., 21 (1976) 2336 [Russ. J. Inorg. Chem., 21 (1976) 1285].
5 P.M. Chukurov, C. Del Pino and B.N. Ivanov-Emin, Zh. Neorg. Khim., 31 (1986) 262 [Russ. J. Inorg. Chem., 31 (1986) 149].
6 C.A. Strydom and C.P.J. Van Vuuren, Thermochim. Acta, 124 (1988) 277.
7 B.N. Ivanov-Emin and Yu.N. Medvedev, Zh. Neorg. Khim., 35 (1990) 300 [Russ. J. Inorg. Chem., 35 (1990) 168].
8 T.J. Taylor, D. Dollimore, G.A. Gamlen, A.J. Barnes and M.A. Stuckey, Thermochim. Acta, 101 (1986) 291.
9 F. Paulik, J. Paulik and M. Arnol, Thermochim. Acta, 121 (1987) 137.
10 A.M. Gadalla and H.-F. Yu, Thermochim. Acta, 164 (1990) 21.
11 C. Popescu, I. Ursu, M. Popescu, R. Alexandrescu, I. Morjan, I.N. Mihailescu and V. Jianu, Thermochim. Acta, 164 (1990) 79.
12 T.J. Taylor, D. Dollimore and G.A. Gamlen, Thermochim. Acta, 101 (1986) 291.
13 M.E. Brown, Introduction to Thermal Analysis, Chapman and Hall, London, 1988, Chap. 13, pp. 131 and 139.
14 B.A. Belov, E.V. Gorozhankin, V.N. Efremov, N.S. Sal'nikova and A.L. Suris, Zh. Neorg. Khim., 30 (1985) 2520 [Russ. J. Inorg. Chem., 30 (1985) 1436].
15 J.A. Anderson, G.J. Millar and C.H. Rochester, J. Chem. Soc. Faraday Trans., 86 (1990) 571.

16 S.J. Conway, J.W. Falconer and C.H. Rochester, J. Chem. Soc. Faraday Trans., 86 (1990) 577.
17 M. Stavola, R.J. Cava and E.A. Rietman, Phys. Rev. Lett., 58 (1987) 1571.
18 B.U. Asanov, O.I. Kondratov, N.V. Porotnikov, and K.I. Petrov, Zh. Neorg. Khim., 33 (1988) 38 [Russ. J. Inorg. Chem., 33 (1988) 21].
19 V.F. Savchenko, L.S. Ivashkevich and I.Ya. Lyudkina, Zh. Neorg. Khim., 33 (1988) 30 [Russ. J. Inorg. Chem., 33 (1988) 17].
20 P. Odier, M. Leblanc and J. Choisnet, Mater. Res. Bull., 21 (1986) 787.
21 A.M. Golub, L.S. Sidoric, S.A. Nedil'ko and T.I. Fedoruk, Izv. Akad. Nauk SSSR, Neorg. Mater., 14 (1978) 1866, [Inorg. Mater., 14 (1978) 1449].
22 J.M. Longo and P.M. Raccah, J. Solid State Chem., 6 (1973) 526.